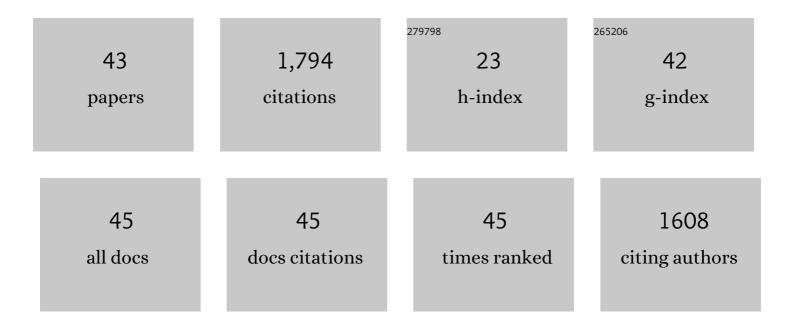
Javier Fullea

List of Publications by Year in descending order

Source: https://exaly.com/author-pdf/4553029/publications.pdf Version: 2024-02-01



INVIED FULLEA

#	Article	IF	CITATIONS
1	Inversion of the satellite observations of the tidally induced magnetic field in terms of 3-D upper-mantle electrical conductivity: method and synthetic tests. Geophysical Journal International, 2022, 229, 2115-2132.	2.4	1
2	On the origin of the Canary Islands: Insights from mantle convection modelling. Earth and Planetary Science Letters, 2022, 584, 117506.	4.4	12
3	Towards a Digital Twin of the Earth System: Geo-Soft-CoRe, a Geoscientific Software & Code Repository. Frontiers in Earth Science, 2022, 10, .	1.8	1
4	Benchmark forward gravity schemes: the gravity field of a realistic lithosphere model WINTERC-G. Solid Earth, 2022, 13, 849-873.	2.8	4
5	WINTERC-G: mapping the upper mantle thermochemical heterogeneity from coupled geophysical–petrological inversion of seismic waveforms, heat flow, surface elevation and gravity satellite data. Geophysical Journal International, 2021, 226, 146-191.	2.4	49
6	A new integrated geophysical-petrological global 3-D model of upper-mantle electrical conductivity validated by the Swarm <i>M</i> 2 tidal magnetic field. Geophysical Journal International, 2021, 226, 742-763.	2.4	2
7	The topography of the Iberian Peninsula from integrated geophysical-petrological multi-data inversion. Physics of the Earth and Planetary Interiors, 2021, 314, 106691.	1.9	6
8	Geodynamic Modeling of Edge-Delamination Driven by Subduction-Transform Edge Propagator Faults: The Westernmost Mediterranean Margin (Central Betic Orogen) Case Study. Frontiers in Earth Science, 2020, 8, .	1.8	12
9	Longâ€Wavelength Gravity Field Constraint on the Lower Mantle Viscosity in North America. Journal of Geophysical Research: Solid Earth, 2020, 125, e2020JB020484.	3.4	2
10	3-D thermochemical structure of lithospheric mantle beneath the Iranian plateau and surrounding areas from geophysical–petrological modelling. Geophysical Journal International, 2020, 222, 1295-1315.	2.4	12
11	Constraining the geotherm beneath the British Isles from Bayesian inversion of Curie depth: integrated modelling of magnetic, geothermal, and seismic data. Solid Earth, 2019, 10, 839-850.	2.8	23
12	Shearâ€Wave Velocity Structure of Southern Africa's Lithosphere: Variations in the Thickness and Composition of Cratons and Their Effect on Topography. Geochemistry, Geophysics, Geosystems, 2018, 19, 1499-1518.	2.5	24
13	Seismic tomography of the Arctic region: inferences for the thermal structure and evolution of the lithosphere. Geological Society Special Publication, 2018, 460, 419-440.	1.3	52
14	Probabilistic Surface Heat Flow Estimates Assimilating Paleoclimate History: New Implications for the Thermochemical Structure of Ireland. Journal of Geophysical Research: Solid Earth, 2018, 123, 10,951.	3.4	4
15	Integrating Gravity and Surface Elevation With Magnetic Data: Mapping the Curie Temperature Beneath the British Isles and Surrounding Areas. Frontiers in Earth Science, 2018, 6, .	1.8	9
16	Hot Upper Mantle Beneath the Tristan da Cunha Hotspot From Probabilistic Rayleighâ€Wave Inversion and Petrological Modeling. Geochemistry, Geophysics, Geosystems, 2018, 19, 1412-1428.	2.5	23
17	On Joint Modelling of Electrical Conductivity and Other Geophysical and Petrological Observables to Infer the Structure of the Lithosphere and Underlying Upper Mantle. Surveys in Geophysics, 2017, 38, 963-1004.	4.6	18
18	Geochemical and geophysical constrains on the dynamic topography of the <scp>S</scp> outhern <scp>A</scp> frican <scp>P</scp> lateau. Geochemistry, Geophysics, Geosystems, 2017, 18, 3556-3575.	2.5	20

JAVIER FULLEA

#	Article	IF	CITATIONS
19	3â€Ð multiobservable probabilistic inversion for the compositional and thermal structure of the lithosphere and upper mantle: III. Thermochemical tomography in the Westernâ€Central U.S Journal of Geophysical Research: Solid Earth, 2016, 121, 7337-7370.	3.4	67
20	Lithospheric structure of Central Europe: Puzzle pieces from Pannonian Basin to Trans‣uropean Suture Zone resolved by geophysicalâ€petrological modeling. Tectonics, 2016, 35, 722-753.	2.8	17
21	A refined model of sedimentary rock cover in the southeastern part of the Congo basin from GOCE gravity and vertical gravity gradient observations. International Journal of Applied Earth Observation and Geoinformation, 2015, 35, 70-87.	2.8	8
22	Perturbing effects of sub-lithospheric mass anomalies in GOCE gravity gradient and other gravity data modelling: Application to the Atlantic-Mediterranean transition zone. International Journal of Applied Earth Observation and Geoinformation, 2015, 35, 54-69.	2.8	27
23	The Canary Islands hot spot: New insights from 3D coupled geophysical–petrological modelling of the lithosphere and uppermost mantle. Earth and Planetary Science Letters, 2015, 409, 71-88.	4.4	37
24	The lithosphere–asthenosphere system beneath Ireland from integrated geophysical–petrological modeling II: 3D thermal and compositional structure. Lithos, 2014, 189, 49-64.	1.4	31
25	The lithosphere–asthenosphere system beneath Ireland from integrated geophysical–petrological modeling — I: Observations, 1D and 2D hypothesis testing and modeling. Lithos, 2014, 189, 28-48.	1.4	22
26	Integrated geophysical-petrological modeling of lithosphere-asthenosphere boundary in central Tibet using electromagnetic and seismic data. Geochemistry, Geophysics, Geosystems, 2014, 15, 3965-3988.	2.5	40
27	Velocity onductivity relations for cratonic lithosphere and their application: Example of Southern Africa. Geochemistry, Geophysics, Geosystems, 2013, 14, 806-827.	2.5	31
28	3â€Ð multiâ€observable probabilistic inversion for the compositional and thermal structure of the lithosphere and upper mantle. II: General methodology and resolution analysis. Journal of Geophysical Research: Solid Earth, 2013, 118, 1650-1676.	3.4	78
29	Integrated geophysical modelling of a lateral transition zone in the lithospheric mantle under Norway and Sweden. Geophysical Journal International, 2013, 194, 1358-1373.	2.4	32
30	3â€Ð multiobservable probabilistic inversion for the compositional and thermal structure of the lithosphere and upper mantle. I: <i>a priori</i> petrological information and geophysical observables. Journal of Geophysical Research: Solid Earth, 2013, 118, 2586-2617.	3.4	121
31	Lithospheric structure in the Baikal–central Mongolia region from integrated geophysicalâ€petrological inversion of surfaceâ€wave data and topographic elevation. Geochemistry, Geophysics, Geosystems, 2012, 13, .	2.5	53
32	Comment on "Deep resistivity cross section of the intraplate Atlas Mountains (NW Africa): New evidence of anomalous mantle and related Quaternary volcanism― Tectonics, 2012, 31, .	2.8	4
33	Water in cratonic lithosphere: Calibrating laboratoryâ€determined models of electrical conductivity of mantle minerals using geophysical and petrological observations. Geochemistry, Geophysics, Geosystems, 2012, 13, .	2.5	63
34	Decoupled crust-mantle accommodation of Africa-Eurasia convergence in the NW Moroccan margin. Journal of Geophysical Research, 2011, 116, .	3.3	30
35	Electrical conductivity of continental lithospheric mantle from integrated geophysical and petrological modeling: Application to the Kaapvaal Craton and Rehoboth Terrane, southern Africa. Journal of Geophysical Research, 2011, 116, .	3.3	66
36	The structure and evolution of the lithosphere–asthenosphere boundary beneath the Atlantic–Mediterranean Transition Region. Lithos, 2010, 120, 74-95.	1.4	126

JAVIER FULLEA

#	Article	IF	CITATIONS
37	Lithospheric structure of the Gorringe Bank: Insights into its origin and tectonic evolution. Tectonics, 2010, 29, n/a-n/a.	2.8	53
38	Effective elastic thickness of Africa and its relationship to other proxies for lithospheric structure and surface tectonics. Earth and Planetary Science Letters, 2009, 287, 152-167.	4.4	142
39	LitMod3D: An interactive 3â€D software to model the thermal, compositional, density, seismological, and rheological structure of the lithosphere and sublithospheric upper mantle. Geochemistry, Geophysics, Geosystems, 2009, 10, .	2.5	107
40	FA2BOUG—A FORTRAN 90 code to compute Bouguer gravity anomalies from gridded free-air anomalies: Application to the Atlantic-Mediterranean transition zone. Computers and Geosciences, 2008, 34, 1665-1681.	4.2	116
41	A rapid method to map the crustal and lithospheric thickness using elevation, geoid anomaly and thermal analysis. Application to the Cibraltar Arc System, Atlas Mountains and adjacent zones. Tectonophysics, 2007, 430, 97-117.	2.2	106
42	The structure of the Atlantic–Mediterranean transition zone from the Alboran Sea to the Horseshoe Abyssal Plain (Iberia–Africa plate boundary). Marine Geology, 2007, 243, 97-119.	2.1	82
43	Lithospheric structure in the Atlantic–Mediterranean transition zone (southern Spain, northern) Tj ETQq1 1 0.7 2006, 338, 140-151.	784314 rgl 1.2	3T /Overlock 38